www.nature.com/aps

Acta Pharmacologica Sinica

ARTICLE

Amuc_1100 pretreatment alleviates acute pancreatitis in a mouse model through regulating gut microbiota and inhibiting inflammatory infiltration

Li-juan Wang[1]✉, Yuan-ling Jin[1], Wen-long Pei[2], Jia-cong Li[1], Rui-lin Zhang[1], Jia-ju Wang[1] and Wei Lin[1,3,4]✉

Amuc_1100 is a membrane protein from *Akkermansia muciniphila*, which has been found to play a role in host immunological homeostasis in the gastrointestinal tract by activating TLR2 and TLR4. In this study we investigated the effects and underlying mechanisms of Amuc_1100 on acute pancreatitis (AP) induced in mice by intraperitoneal injection of caerulein and lipopolysaccharide (LPS). The mice were treated with the protein Amuc_1100 (3 μg, i.g.) for 20 days before caerulein injection. Cecal contents of the mice were collected for 16S rRNA sequencing. We found that pretreatment with Amuc_1100 significantly alleviated AP-associated pancreatic injury, reduced serum amylase and lipase. Amuc_1100 pretreatment significantly inhibited the expression of proinflammatory cytokines (TNF-α, IL-1β, IFN-γ and IL-6) in spleen and pancreas through inhibiting NF-κB signaling pathway. Moreover, Amuc_1100 pretreatment significantly decreased the inflammatory infiltration, accompanied by the reduction of $Ly6C^{+}$ macrophages and neutrophils in the spleen of AP mice. Gut microbiome analysis showed that the abundance of *Bacteroidetes*, *Proteobacteria*, *Desulfobacterota* and *Campilobacterota* was decreased, while the proportion of *Firmicutes* and *Actinobacteriota* was increased in AP mice pretreated with Amuc_1100. We further demonstrated that Amuc_1100 pretreatment restored the enrichment of tryptophan metabolism, which was mediated by intestinal flora. These results provide new evidence that Amuc_1100 lessens the severity of AP through its anti-inflammatory properties with a reduction of macrophages and neutrophil infiltration, as well as its regulation of the composition of intestinal flora and tryptophan metabolism.

Keywords: acute pancreatitis; Amuc_1100; inflammation; gut microbiota; tryptophan metabolism

Acta Pharmacologica Sinica (2024) 45:570–580; https://doi.org/10.1038/s41401-023-01186-4

INTRODUCTION

Acute pancreatitis (AP) is a complex disease characterized by an acute inflammatory process of the pancreas that can progress from manageable and mild inflammation to multiple organ failure if left untreated [1]. In its early stages, AP is not easily detected. However, approximately 80 percent of patients develop moderate to severe pancreatitis [2, 3]. The mortality rate of severe pancreatitis is as high as 20% under modern medical conditions [2, 4, 5]. Clinically, AP is diagnosed by the presence of at least two of three characteristics: abdominal pain, elevated pancreatic enzymes including amylase and lipase, and typical images of computerized tomography (CT) or magnetic resonance imaging (MRI) [6]. Excessive alcohol consumption (approximately 30% of cases) and cholelithiasis (approximately 35%–40% of cases) are the two leading causes of AP [7]. Other etiologies of AP include hypertriglyceridemia, hypercalcemia, hereditary pancreatitis, viral infections, pancreas injuries, tumors, and cystic lesions. Based on severity grading, AP can be classified as mild, moderately severe, and severe [8]. Treatment of AP includes medication, fluid management, nutrition and risk-reduction strategies [1].

The failure of gut barrier function, resulting in increased mucosal permeability, may lead to the translocation of intestinal bacteria during AP. Accumulating evidence suggests the possible involvement of the gut microbiome in AP [9]. The gut microbial composition is critical in regulating immune responses to defend against invasive pathogens [10]. Interventions that modulate the host-microbiome community eliminate harmful bacteria and reconstitute beneficial flora [11, 12]. In AP patients, *Enterobacteriaceae* and *Firmicutes* increased, while *Bacteroidetes* and *Lactobacillus* were reduced. The elevation of serum IL-6 was positively correlated to *Enterobacteriaceae* and *Enterococcus*, and negatively correlated to the cluster number of *Bifidobacterium* and *Clostridium* [13]. The reduction of proinflammatory factors, including IL-1β, TNF-α, CXCL1, and IL-18, was related to altering specific commensal bacteria, and inversely associated with pancreatitis severity and systemic infection [14]. Furthermore, the ratio of *Firmicutes* to *Bacteroides* increased obviously with an augment of *Firmicutes* and a reduction of *Bacteroidetes*, *Alloprevotella*, *Blautia*, *Gemella* and *Bifidobacterium* in the intestinal microbiota compared to healthy control. However, the abundances of *Proteobacteria*,

[1]Department of Pathogen Biology, School of Medicine and Holistic Integrative Medicine, Nanjing University of Chinese Medicine, Nanjing 210023, China; [2]Center for Global Health, School of Public Health, Nanjing Medical University, Nanjing 211166, China; [3]State Key Laboratory of Bioreactor Engineering, East China University of Science and Technology, Shanghai 200237, China and [4]State Key Laboratory of Drug Research, Shanghai Institute of Materia Medica, Chinese Academy of Sciences, Shanghai 201203, China
Correspondence: Li-juan Wang (lucywang2012@163.com) or Wei Lin (weilin@njucm.edu.cn)
These authors contributed equally: Li-juan Wang, Yuan-ling Jin, Wen-long Pei

Received: 24 April 2023 Accepted: 20 October 2023
Published online: 27 November 2023

SPRINGER NATURE © The Author(s), under exclusive licence to Shanghai Institute of Materia Medica, Chinese Academy of Sciences and Chinese Pharmacological Society 2023

Escherichia Shigella, *Enterococcus*, *Acinetobacter*, *Stenotrophomonas* and *Geobacillus*, were over-represented in these patients [15]. These studies indicate that restoring physiological intestinal flora homeostasis and stabilizing the gut barrier are valuable strategies for AP treatment.

Amuc_1100 is a membrane protein from *Akkermansia muciniphila* (*A. muciniphila*) that has been shown to interact with Toll-like receptor 2 (TLR2) and improve the gut barrier and metabolism in obese and diabetic mice [16]. Additionally, Amuc_1100 has been found to play a role in host immunological homeostasis in the gastrointestinal tract by activating TLR2 and TLR4 to promote high levels of IL-10 [17]. Supplementation with Amuc_1100 has been shown to reduce dyslipidemia, insulin resistance and fat mass development [18], as well as improve colitis by decreasing the number of infiltrating $CD8^+$ T cells and macrophages in the colon of mice. Moreover, Amuc_1100 mitigated tumorigenesis by expanding the number of $CD8^+$ T cells in the mesenteric lymph nodes and secreting high levels of TNF-α [19]. Due to its anti-inflammatory properties, particularly macrophage polarization, Amuc_1100 has also been effective in managing periodontitis [20]. Furthermore, Amuc_1100 directly interacted with TLR2 to improve extracellular availability and 5-HT biosynthesis [21]. Some of the beneficial effects of *A. muciniphila* on host metabolism were partially replicated by Amuc_1100 [22], making it a promising candidate for future drug development [23]. However, the function and mechanism by which Amuc_1100 improves the gut microbiota and metabolism in a mouse model of AP remains unclear. Therefore, we aimed to investigate whether Amuc_1100 improves gastrointestinal microbe and metabolic balance during AP.

In this study, we found that Amuc_1100 treatment significantly decreased pathological damage to the pancreas, as well as levels of serum amylase and lipase in a mouse model of AP. Moreover, oral supplementation with Amuc_1100 reduced the proportion of proinflammatory macrophages and neutrophils in the spleen via the NF-κB signaling pathway. To investigate the potential mechanism behind these effects, we used 16S rRNA gene sequencing to analyze the gut microbiota in cecal contents from the control, AP and AP+Amuc_1100 groups. Our results demonstrated significant changes in the composition of gut microbiota. Additionally, we observed significant alterations in the metabolic profiles of serum.

MATERIALS AND METHODS

Expression and purification of Amuc_1100 in vitro

The plasmid pET-26b-Amuc_1100 was constructed using the pET-26b (+) vector as a template. According to a prior publication, pET-26b-Amuc_1100 was transformed into *Escherichia coli* BL21 (DE) [19]. The expression of Amuc_1100 in BL21 cells was induced by adding 1 mM isopropyl-β-d-thiogalactoside (IPTG) during the log phase of growth. Bacteria were lysed and their lysate was used to purify the Amuc_1100 protein, using a protocol from Novagen for Ni-HTA resin (Merck Millipore, USA). Purified proteins, as well as crude lysate, were resolved via SDS-PAGE, and the results of Coomassie brilliant blue staining (Supplementary Fig. 1a) followed by Western blotting (Supplementary Fig. 1b) indicated that Amuc_1100 was successfully expressed and purified in vitro. The concentration of Amuc_1100 was determined using a BCA Protein Kit (Beyotime, China). Aliquots of purified Amuc_1100 were stored at −80 °C.

Animal experiments

All experimental protocols of mice followed the guidelines for the care and use of laboratory animals of Nanjing University of Chinese Medicine and approved by the animal welfare committee of Nanjing University of Chinese Medicine. Male C57BL/6J mice aged between 6 and 8 weeks were randomly divided into three groups (Control, AP, AP+Amuc_1100) and raised under specific pathogen-free (SPF) conditions with a 12- h/12-h dark/night cycle. All mice had access to food and water under controlled temperature (22–24 °C) and humidity (50%–55%) conditions. Body weight was obtained daily. Mice in the AP and AP +Amuc_1100 groups were intraperitoneally injected with caerulein (50 μg/kg body weight, 10 times at 1-h intervals) (Shanghai Yuanye Bio-Technology Co., Ltd, China) and lipopolysaccharide (LPS, 5 mg/kg body weight, at the same time as the caerulein injection) (Sigma-Aldrich, USA), both of which were dissolved in sterile normal saline (NS). To explore the effects of Amuc_1100 on AP, mice were treated with an oral administration of the protein Amuc_1100 (3 μg) in an equivalent volume of sterile phosphate buffer saline (PBS) containing 2.5% glycerol beginning 20 days before caerulein injection. All mice were sacrificed 1 h after LPS injection. The spleen, liver, kidney and pancreatic tissues were isolated and weighed. Blood and cecal contents were collected for further analysis. A schematic diagram of the experimental design is depicted in Supplementary Fig. 2.

Histological analysis and immunohistochemistry (IHC)

For histological assessment, pancreatic tissue was fixed, dehydrated and embedded in paraffin. The embedded paraffin sections were sliced to a thickness of 3 μm. Thereafter, these sections were stained with hematoxylin and eosin (H&E). For IHC assays, the paraffin sections were deparaffinized, endogenous enzymes were inactivated and antigens were thermally repaired. The sections were then blocked and stained with F4/80 or Ly6G antibody, followed by corresponding secondary antibody and a Streptavidin Biotin Complex kit (Boster BioEngineering, China). The detailed information of antibodies for IHC analysis is listed in Supplementary Table 2. Finally, morphology and structure of the stained sections were observed under a microscope (Zeiss, Germany). The pancreatic histological score was calculated by edema, inflammation, hemorrhage, and necrosis according to a previous study [24]. IHC was quantified by Image-Pro-Plus software and the mean density was determined based on the rate of integral optical density sum and area.

Measurement of serum amylase and lipase

The blood of sacrificed mice was allowed to stand for 2 h at room temperature and centrifuged at 4000 rpm for 10 min at 4 °C. The serum was collected as the supernatant of this centrifugation. The amylase and lipase levels in the supernatant were measured using a Roche Cobas c 701/702 (Roche Diagnostics) alongside commercial kits (Roche, Switzerland).

RNA extraction and quantitative real-time polymerase chain reaction (qPCR)

Pancreatic and splenic tissues of mice were collected and subsequently flash-frozen in liquid nitrogen. Total RNA was isolated from pancreatic or splenic tissue using TRIzol (TIANGEN, China) according to the manufacturer's instructions. Collected RNA was reverse transcribed into cDNA using HiScript II Q RT SuperMix (Vazyme, China). qPCR was then conducted on cDNA using SYBR-Green (Vazyme, China) and LightCycler96 System (Roche, Switzerland). The specific primers used for qPCR are listed in Supplementary Table 1. The housekeeping gene GAPDH was used as an internal reference gene.

Western blot assay

The spleen and pancreas were cryogenically ground in liquid nitrogen and lysed in RIPA buffer supplemented with protease and phosphatase inhibitors. The concentration of protein in the spleen and pancreas was measured using a BCA protein kit (Beyotime, China). After heating to 100 °C for 10 min, an equal amount of protein was separated by SDS-PAGE. The protein on the gel was transferred to PVDF membranes. The PVDF

membranes were placed in 5% bovine serum albumin for 2 h at room temperature to block non-specifically bound proteins. The primary antibody was incubated overnight at 4 °C and the secondary antibody was incubated at room temperature for 1 h. All antibodies used are outlined in Supplementary Table 2. The protein bands were developed using a chemiluminescence kit (Beyotime, China). The band density was observed using Image Lab. Relative protein levels were standardized to an internal reference β-Tubulin.

Macrophage and neutrophil detection by flow cytometry (FCM)
To prepare single-cell suspensions, freshly harvested spleens were divided into pieces, ground and filtered through a 70 μm nylon mesh. Cells were resuspended in PBS containing 2% fetal bovine serum, and blocked with Purified Rat Anti-Mouse CD16/CD32 (BD Biosciences) for 15 min at room temperature. Single-cell suspensions were stained with Zombie NIR™ Fixable Viability Kit (BioLegend) for 15 min at room temperature. For macrophage identification, mononuclear cells were stained with PE/Cyanine7 anti-mouse F4/80 Antibody (BioLegend), FITC anti-mouse/human CD11b Antibody (BioLegend), PerCP/Cyanine5.5 anti-mouse Ly6C Antibody (BioLegend), and PE/Dazzle™ 594 anti-mouse CD279 (PD-1) Antibody (BioLegend) for 30 min at 4 °C, protected from light. For neutrophil analysis, splenocytes were stained with PE/Cyanine7 anti-mouse F4/80 Antibody (BioLegend), FITC anti-mouse/human CD11b Antibody (BioLegend), PE anti-mouse Ly6G Antibody (BioLegend), PE/Dazzle™ 594 anti-mouse CD279 (PD-1) Antibody (BioLegend) for 30 min at 4 °C, and protected from light. The data processing was handled using FlowJo_V10.

16S rRNA gene sequencing
The cecal contents obtained from mice were frozen in liquid nitrogen until use. Microbial DNA from cecal contents was isolated and then 16S rRNA was amplified, targeting the hypervariable region. The purified amplicon sequences were detected by Illumina MiSeq (PE300). The data were analyzed by Majorbio Bio-pharm Biotechnology (www.i-sanger.com).

Serum metabolites and data processing
Thawed serum samples (50 μL) were spiked with ice-cold methanol (200 μL) and then centrifuged at 12,000 × *g* for 15 min at 4 °C. The supernatant was detected using a Dionex Ultimate 3000 UPLC system coupled with a Q-Orbitrap-MS (Q-Exactive plus MS, Thermo Fisher Scientific) with a heated-electrospray ionization source. Quality control (QC) samples were used for stability and repeatability. For quantification of Trp metabolites, ten microlitres of Trp-d5 (1 mg/L) was added as the internal standard. Chromatographic separation was performed on a Hypersile C18 column with a 100 mm × 2.1 mm particle diameter at 40 °C. The mobile phases comprised ultra-pure water with 0.1% formic acid and acetonitrile with 0.1% formic acid. The flow rate of the mobile phase was 0.4 mL/min with a linear-gradient elution procedure. The UPLC automatic sampler had a temperature and volume of 4 °C and 5 μL, respectively. The MS conditions were set as follows: positive and negative ion mode; spray voltage of 3 kV; capillary ion transport tube temperature, 300 °C; sheath gas flow rate, 50 au; auxiliary gas flow rate, 10 au; purge gas flow rate, 2 au; full scanning ion range, 70–800 amu.

Raw data were processed with SIEVE software (Thermo Fisher Scientific, USA). After base peak correction, background subtraction and deconvolution of each sample through TraceFinder (Thermo Fisher Scientific, USA), the data table containing an exact mass number, retention time and peak area of ions was obtained. Qualitative analysis was then conducted using the Human Metabolome Database (HMDB) alongside the METLIN database. Principal component analysis (PCA) and partial least squares discriminant analysis (PLS-DA) were performed after importing the normalized values into SIMCA-P 14.1 software. MetaboAnalyst and KEGG were used for pathway analysis. For quantification of Trp metabolites, data acquisition and analysis were performed with the Thermo XCalibur 2.2 software.

Statistical analysis
Data are shown as the mean ± SEM. Differences across the three groups were analyzed by one-way ANOVA with Tukey's multiple comparisons test. *P* values of less than 0.05 ($P < 0.05$) were considered statistically significant. All experiments were independently repeated at least three times.

RESULTS

Oral administration of Amuc_1100 alleviated pancreatic injury in AP mice
The body weights of mice in the three groups showed no significant differences (Supplementary Fig. 3a). However, AP mice exhibited increased weights in their pancreas, lung and kidney tissues, which were reduced by oral administration of Amuc_1100 (Fig. 1a and Supplementary Fig. 3b, c). To investigate the effects of Amuc_1100 on the pancreas in AP mice, pancreas pathology was observed by H&E staining. Results showed that AP mice displayed aggravated degrees of inflammatory cell infiltration, edema, hemorrhage, and acinar necrosis compared to the control group. Nevertheless, Amuc_1100 treatment significantly attenuated the histological injury in the pancreas of mice (Fig. 1b), as evidenced by the histologic scores (Fig. 1c). Moreover, AP mice exhibited significantly increased serum levels of amylase and lipase, which were reduced considerably by Amuc_1100 treatment (Fig. 1d, e). To evaluate the degree of inflammation in AP, proinflammatory cytokines (TNF-α, IL-1β, IFN-γ, IL-6) and anti-inflammatory factors (IL-4, IL-10, TGF-β1) were detected through qPCR of the pancreatic tissues (Fig. 1f–l). Results showed high levels of proinflammatory cytokines and low levels of anti-inflammatory factors released in the AP group. However, oral supplementation of Amuc_1100 alleviated pancreatic inflammation. The primary regulator of innate immunity is the NF-κB signaling pathway, which is involved in inflammation regulation in AP mice [25, 26]. Western blot analysis of the pancreatic tissues showed that relative protein levels of TLR2, IKKα, IKBα, NF-κB p65 and Phospho-NF-κB p65 increased in the AP group compared to the control group, while oral supplementation of Amuc_1100 reversed this phenomenon (Fig. 1m). It suggested that Amuc_1100 intervention could mitigate pancreatic inflammation in AP mice through NF-κB pathway. Overall, these findings demonstrated that oral administration of Amuc_1100 markedly alleviated the severity of AP.

Supplementation with Amuc_1100 enhanced anti-inflammatory properties in AP mice
To investigate the effects of Amuc_1100 treatment on systemic inflammation in AP mice, spleen indices were measured. Results indicated that spleen weights were heavier in AP mice than control mice, but oral supplementation with Amuc_1100 alleviated splenomegaly in AP mice (Fig. 2a). Furthermore, alterations in proinflammatory cytokines and anti-inflammatory factors were observed in the spleen tissues of mice with AP compared to those in the control group. This was supported by elevated levels of TNF-α (Fig. 2b), IL-1β (Fig. 2c), IFN-γ (Fig. 2d), and IL-6 (Fig. 2e), as well as reduced levels of IL-4 (Fig. 2f), IL-10 (Fig. 2g), and TGF-β1 (Fig. 2h). However, subsequent qPCR analyses of AP mice treated with Amuc_1100 demonstrated a significant reversal of the aforementioned inflammatory factors. Western blot analysis of the spleen demonstrated that relative protein levels of IKKβ, IKBα, NF-κB p65 and Phospho-NF-κB p65 increased in the AP group compared to the control group. However, Amuc_1100 treatment reduced these increases. Conversely, relative protein level of IKKα was decreased in the AP group compared to the control group, but Amuc_1100 treatment upregulated the level (Fig. 2i). These

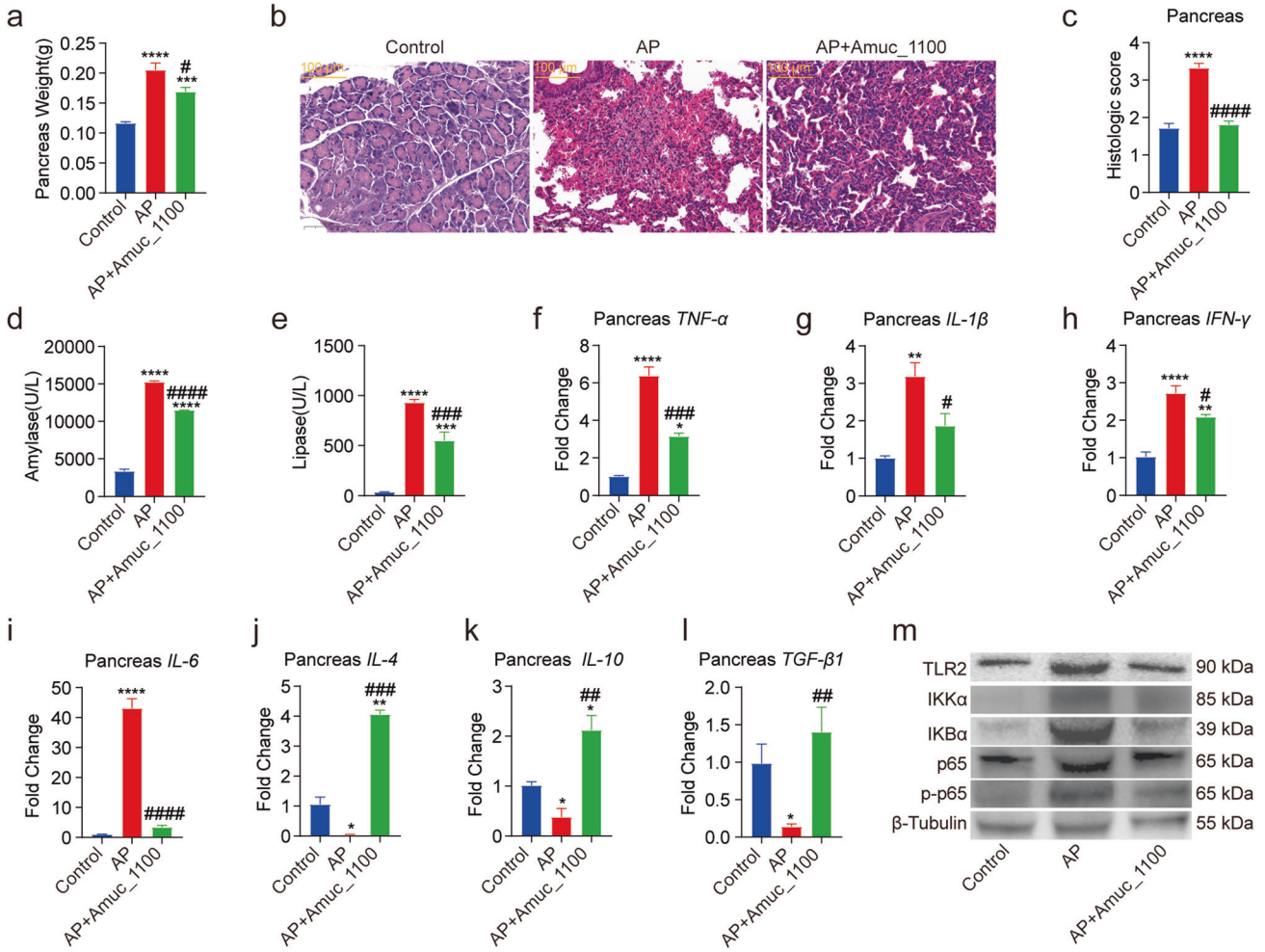

Fig. 1 Amuc_1100 treatment protected against pancreatic degradation of AP mice. a Pancreas weight analysis. **b** Representative images showed Amuc_1100 gavage significantly decreased morphological damage in the form of inflammatory infiltration and necrosis in AP mice. All images were generated at 200× amplification. Scale bars, 100 μm. **c** Pathological scores of pancreases among control, AP and AP +Amuc_1100 groups. The serum levels of amylase (**d**) and lipase (**e**). The mRNA expression of proinflammatory cytokines in the pancreas, including *TNF-α* (**f**), *IL-1β* (**g**), *IFN-γ* (**h**), and *IL-6* (**i**). Levels of anti-inflammatory cytokine mRNA were analyzed using quantitative real-time PCR (qPCR), such as *IL-4* (**j**), *IL-10* (**k**), and *TGF-β1* (**l**). **m** Western blot was used to measure NF-κB signaling pathway and TLR2 expression among three groups. β-tubulin was used as an internal standard. Data are provided as the mean ± SEM and were analyzed by one-way ANOVA and Tukey's multiple comparisons test. $^{*}P < 0.05$; $^{**}P < 0.01$ $^{***}P < 0.001$, $^{****}P < 0.0001$, compared with Control. $^{\#}P < 0.05$; $^{\#\#}P < 0.01$, $^{\#\#\#}P < 0.001$; $^{\#\#\#\#}P < 0.0001$, compared to AP mice.

results further confirmed the protective effects of Amuc_1100 supplementation in AP mice.

Amuc_1100 treatment reduced macrophage and neutrophil infiltration in AP mice

To investigate the impact of Amuc_1100 treatment on splenic inflammation in AP mice, we examined the proportion of macrophages and neutrophils and the expression level of PD-1 using flow cytometry (Supplementary Fig. 4). Infiltration of macrophages and neutrophils has increased the gene expression of proinflammatory cytokines such as TNF-α, IL-1β, and IL-6 [27]. We found that the percentage of macrophages was significantly increased in the spleens of AP mice, while Amuc_1100 treatment significantly decreased this percentage (Fig. 3a). However, the proportion of PD-1^{+} macrophages did not change in the spleen, regardless of Amuc_1100 supplementation (Fig. 3b). Additionally, the proportion of Ly6C^{+} macrophages was significantly elevated in the AP group compared to the control group, and Amuc_1100 treatment inhibited this elevation (Fig. 3c). However, oral administration of Amuc_1100 did not impact the expression of PD-1 on Ly6C^{+} macrophages in the spleen (Fig. 3d). Moreover, Amuc_1100 treatment alleviated splenic infiltration of neutrophils (Fig. 3e). Interestingly, the percentage of PD-1^{+} neutrophils was significantly reduced, but Amuc_1100 supplementation reversed this phenomenon (Fig. 3f). Furthermore, Amuc_1100 treatment suppressed the pancreatic infiltration of macrophages and neutrophils in AP mice (Fig. 3g). Taken together, our results demonstrate that oral administration of Amuc_1100 markedly attenuated splenic and pancreatic inflammation in AP mice.

Amuc_1100 modulated the composition of gut microbiota in AP mice

To explore the relationship between gut microbiota and the progression of AP and the effect of Amuc_1100 treatment, we analyzed the abundance and composition of intestinal flora in cecal contents among the control, AP and AP+Amuc_1100 groups using 16S rRNA sequencing. Rarefaction curves indicated near-complete sampling of the community (Supplementary Fig. 5a). The community richness, based on Sobs, Ace and Chao indices, was not significantly altered among the three groups (Fig. 4a).

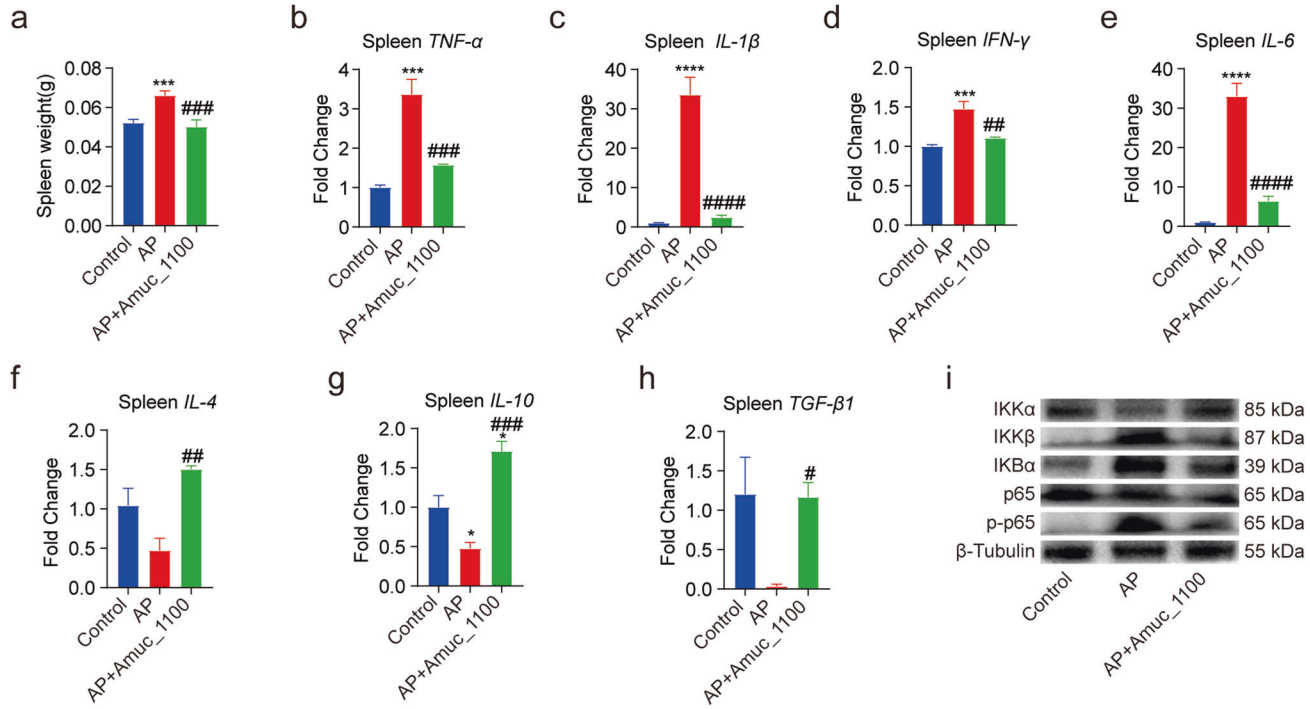

Fig. 2 Supplementation with Amuc_1100 improved AP induced by caerulein and LPS. a Spleen weight analysis. The mRNA expression of *TNF-α* (**b**), *IL-1β* (**c**), *IFN-γ* (**d**), *IL-6* (**e**), *IL-4* (**f**), *IL-10* (**g**), *TGF-β1* (**h**) in the spleen were detected by qPCR. **i** Protein lysates were evaluated under the same experimental conditions in the spleen. Immunoblot assay of the expression of the NF-κB signaling with antibodies specific for IKKα, IKKβ, IKBα, p65 and p-p65. β-Tubulin was employed as an internal control. Data are provided as the mean ± SEM and were analyzed by one-way ANOVA and Tukey's multiple comparisons test. $^{***}P < 0.001$; $^{****}P < 0.0001$, compared with Control. $^{\#}P < 0.001$; $^{\#\#}P < 0.01$; $^{\#\#\#}P < 0.001$; $^{\#\#\#\#}P < 0.0001$, compared to AP mice.

However, PLS-DA analysis of sequencing data shows clear separation of community composition among the groups (Fig. 4b). At the genus level, Venn diagrams revealed six unique operational taxonomic units (OTUs) in control mice and one unique OTU in both AP induction and Amuc_1100 intervention mice (Supplementary Fig. 5b). LEfSe analysis generated cladograms and LDA scores, revealing differences in taxa from the phylum level to the genus level among the three groups (Supplementary Fig. 5c, d).

We analyzed the relative abundances of phyla in microbial communities among the three groups to identify differences. The results showed that the abundance of *Firmicutes* decreased in mice with AP in comparison to controls, while it tended to increase in AP mice after Amuc_1100 treatment (Fig. 4c). The abundance of *Bacteroidetes*, the predominant phylum, increased dramatically in AP mice compared to controls, whereas the proportion of *Bacteroidota* was reduced in Amuc_1100-treated mice relative to AP mice (Fig. 4d). Consistently, Amuc_1100-treated mice exhibited a robustly increased *Firmicutes*/*Bacteroidota* ratio (Fig. 4e) as well as *Actinobacteriota* abundance (Fig. 4f). Additionally, the phyla *Proteobacteria* (Fig. 4g), *Desulfobacterota* (Fig. 4h) and *Campilobacterota* (Fig. 4i) were relatively abundant in the AP group, but their abundance decreased after oral administration of Amuc_1100 in AP mice. These findings suggest that Amuc_1100 treatment improved gut dysbiosis in the mice with AP induction.

Amuc_1100 intervention altered metabolic profiling of serum in AP mice

PLS-DA analysis revealed apparent differences among the control, AP and AP + Amuc_1100 groups (Fig. 5a). In AP mice, we identified 19 differential metabolites in serum. After Amuc_1100 treatment, serum metabolomics showed 18 differential metabolites (Fig. 5b). KEGG enrichment analysis showed that tryptophan metabolism, arginine and proline metabolism, linoleic acid metabolism, primary bile acid biosynthesis were enriched (Supplementary Fig. 6a, b). The data confirmed that tryptophan metabolism was the only enriched pathway with significant differences in serum among all three groups (Fig. 5c, d). Specifically, *L*-tryptophan (Trp) and serotonin (5-hydroxytryptamine, 5-HT) had lower abundance in AP mice than controls. However, Amuc_1100 supplementation increased the serum levels of Trp (Fig. 5e) and 5-HT (Fig. 5f) in AP mice.

Integration of metagenomes and metabolomes in AP mice with Amuc_1100 treatment

We integrated both 16S rRNA and metabolomic data into multiomic features. Among the metabolites involved in the tryptophan metabolism pathway, indolelactic acid levels were positively correlated with nine genera and negatively correlated with two genera. *L*-tryptophan levels were positively correlated with two genera and negatively correlated with 11 genera. We performed network analysis based on integrating 16S rRNA sequencing and metabolomic results to investigate the relationship between the microbiome and AP-linked metabolites. The data showed that the abundances of *Parabacteroides*, *Roseburia*, *Desulfovibrionaceae* and *Ruminococcaceae* were positively correlated with indolelactic acid, but negatively correlated with *L*-tryptophan levels (Fig. 6).

Effects of Amuc_1100 on Trp metabolic profiling in mice with AP

To determine whether Amuc_1100 regulates Trp metabolism, metabolomic profiling was applied to compare the global metabolites in AP mice with or without Amuc_1100 treatment. AP mice significantly increased the serum levels of 5-HTP, 5-HIAA, Kyn, PA, QA, IAld, IAAld and IA. In contrast, Amuc_1100 supplementation normalized the serum levels of them (Fig. 7a–l). AP mice significantly increased the feces levels of tryptamine, IAAld and the pancreas levels of 5-HTP, Kyn, QA, IAAld, IA, while reduced the feces levels of 5-HIAA, Kyn, PA, QA, IAld, IA, IPA and the pancreas levels of *L*-Trp (Fig. 7m–af). Oral administration of Amuc_1100 in AP

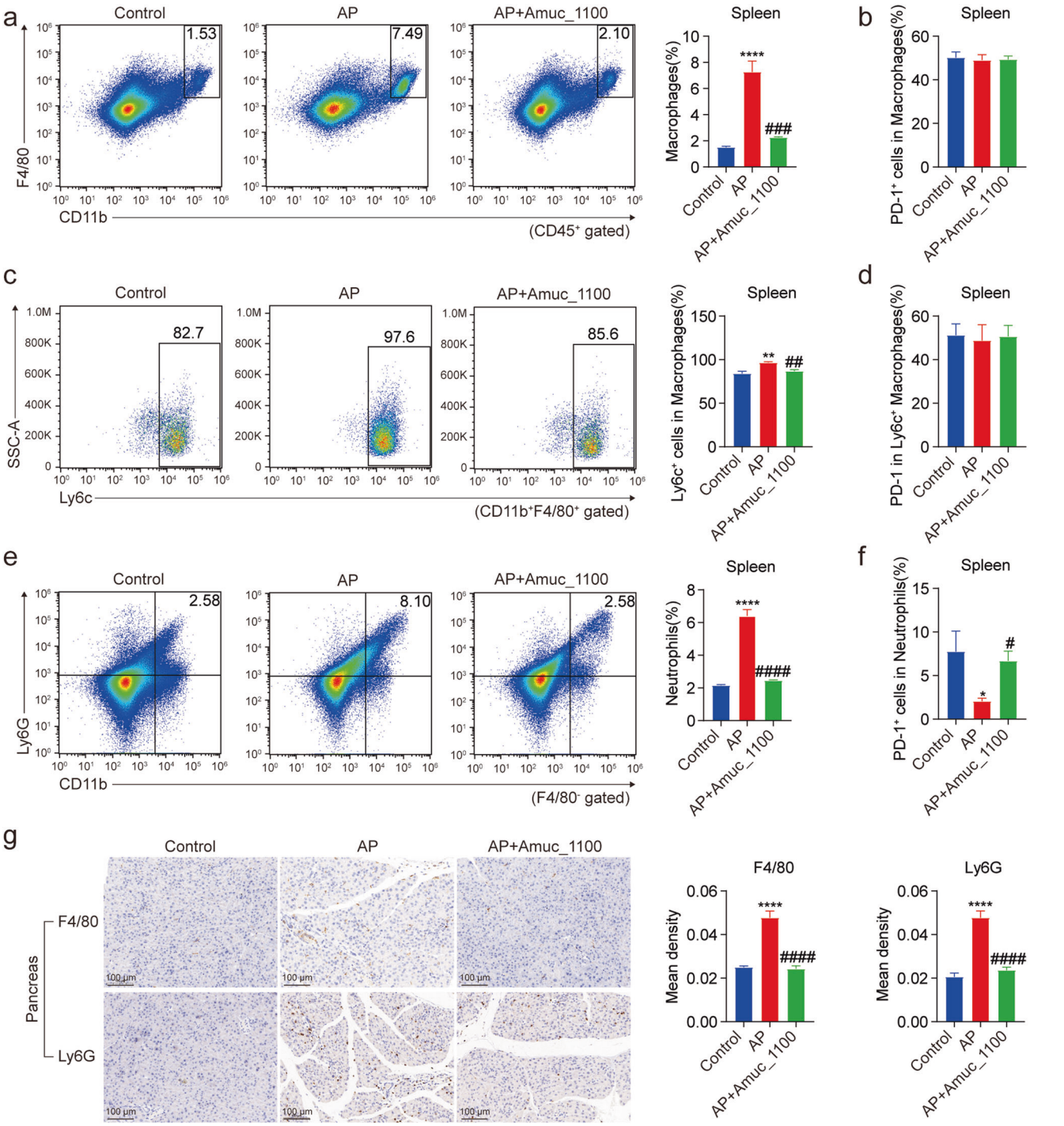

Fig. 3 The effect of Amuc_1100 on macrophage and neutrophil infiltration in AP mice. Scatter plot analysis of the percentage of $CD11b^{+}F4/80^{+}$ cells in lymphocytes and quantification of macrophages (**a**), $PD\text{-}1^{+}$ macrophages (**b**), $Ly6c^{+}$ macrophages (**c**), $PD\text{-}1^{+}Ly6c^{+}$ macrophages (**d**), neutrophils (**e**) and $PD\text{-}1^{+}$ neutrophils (**f**) in the spleen. **g** IHC staining and quantitation of F4/80 and Ly6G in the pancreatic tissue. Scale bars, 100 μm. Data are provided as the mean ± SEM and were analyzed by one-way ANOVA and Tukey's multiple comparisons test. $^{*}P < 0.05$; $^{**}P < 0.01$; $^{****}P < 0.0001$, compared with Control. $^{\#}P < 0.05$; $^{\#\#}P < 0.01$; $^{\#\#\#\#}P < 0.0001$, compared to AP mice.

mice could reverse this phenomenon through AhR (Fig.7ag). These data indicated that Amuc_1100 could regulate Trp metabolism in AP mice targeting AhR.

DISCUSSION

According to the revised Atlanta grading criteria, a diagnosis of AP requires the fulfillment of at least two of the following three criteria: abdominal pain, serum amylase and/or lipase greater than three times the upper limit of normal, and CT or MRI images that coincide with AP [6]. Management of AP involves two conditions: fluid resuscitation to maintain or restore tissue perfusion, nutritional support to reduce infectious rate and counter decomposition [8]. In the present experiment, the AP mice model was established by intraperitoneal injection of caerulein and LPS, resulting in pathological injury in pancreatic

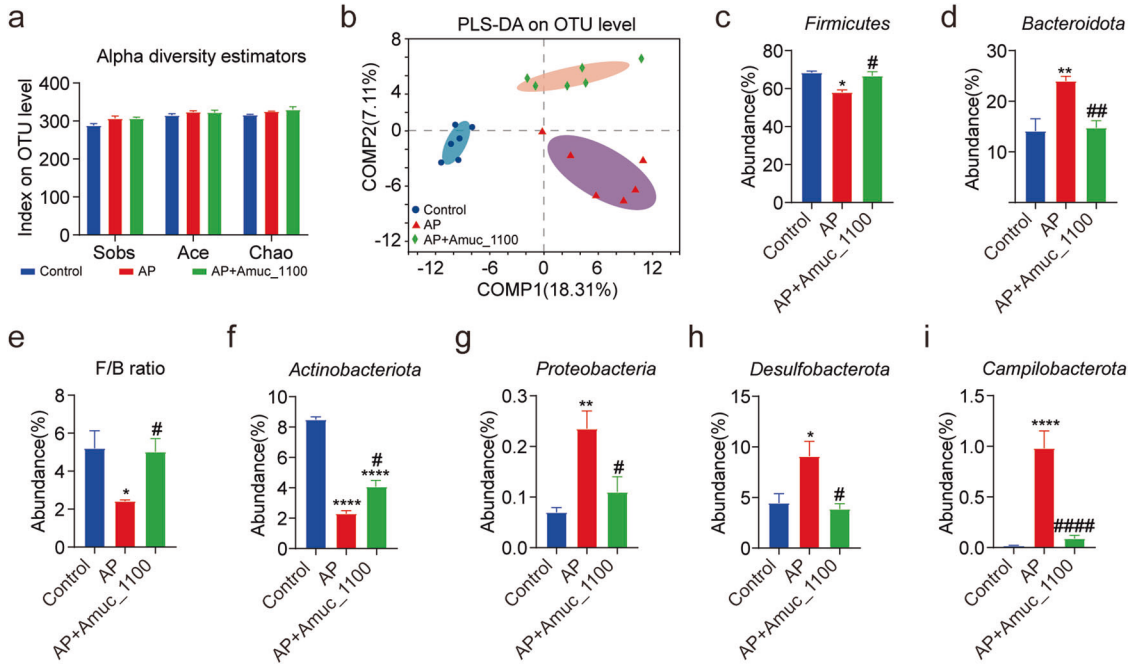

Fig. 4 Bacterial abundance and community composition differences across control, AP, and AP+Amuc_1100 groups. 16S rRNA gene sequencing was performed on cecal contents obtained from mice to analyze the abundance and microbiome composition. **a** Alpha diversity indicators (Sobs, Ace, Chao) and **b** Partial Least-Squares Discriminant Analysis (PLS-DA) among control, AP and AP+Amuc_1100 groups. *Firmicutes* (**c**), *Bacteroidota* (**d**), *Firmicutes/Bacteroidota* ratio (**e**), *Actinobacteriota* (**f**), *Proteobacteria* (**g**), *Desulfobacterota* (**h**), *Campilobacterota* (**i**) of the three groups. Data are provided as the mean ± SEM and were analyzed by one-way ANOVA and Tukey's multiple comparisons test. $^{*}P < 0.05$; $^{**}P < 0.01$; $^{****}P < 0.0001$, compared with Control. $^{\#}P < 0.05$; $^{\#\#}P < 0.01$; $^{\#\#\#\#}P < 0.0001$, compared to AP mice.

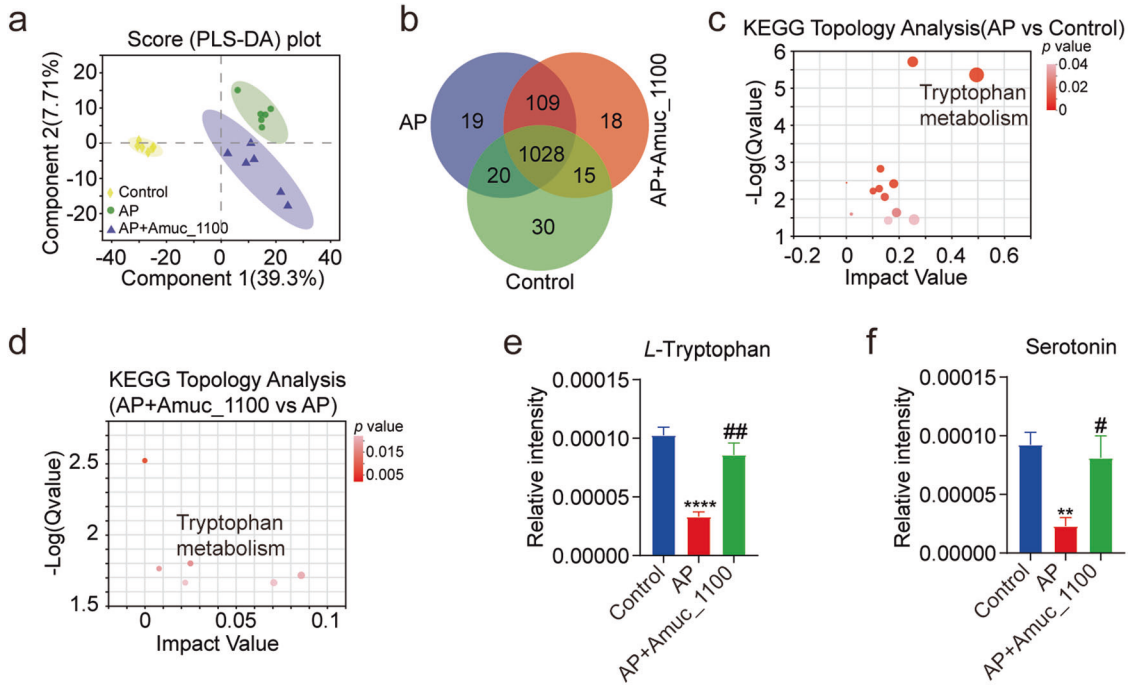

Fig. 5 Metabolic profiling of serum in mice. a PLS-DA score among control, AP and AP+Amuc_1100 groups. **b** Differentially expressed metabolites are represented in a Venn diagram for the three groups. **c** Pathway analysis of differential metabolites between control and AP groups. **d** Pathway analysis of differential metabolites in AP mice upon Amuc_1100 administration. The effects of Amuc_1100 on levels of *L*-tryptophan (**e**) and serotonin (**f**) in serum of mice with AP. Data are provided as the mean ± SEM and were analyzed by one-way ANOVA and Tukey's multiple comparisons test. $^{**}P < 0.01$; $^{****}P < 0.0001$, compared with Control. $^{\#}P < 0.05$; $^{\#\#}P < 0.01$, compared to AP mice.

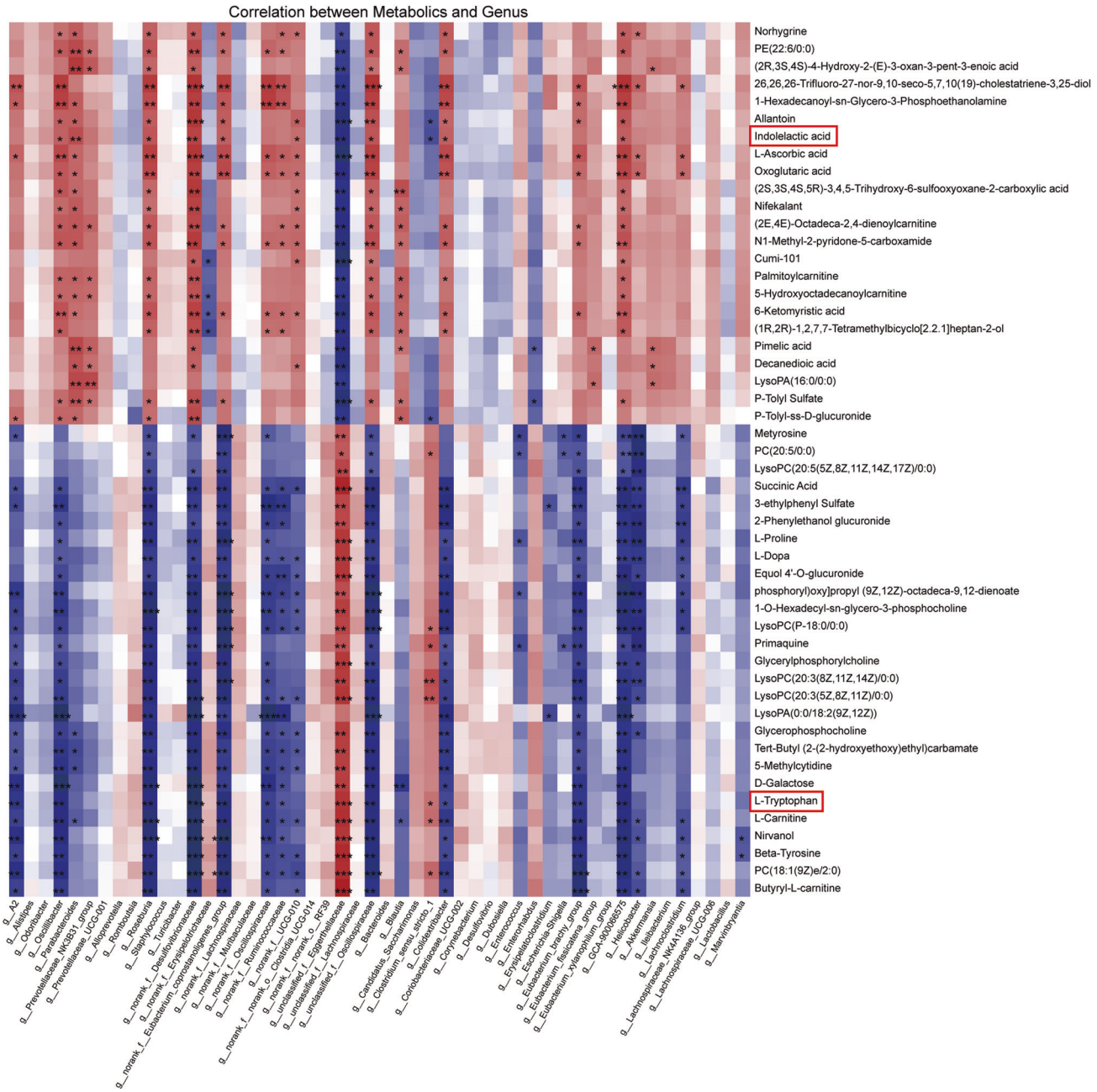

Fig. 6 AP-associated genera correlate with metabolites which differentiate mice with AP and Amuc_1100 intervention. The genera and serum metabolites possess significant differences between the AP + Amuc_1100 and AP groups. Significant correlations are denoted by asterisks (*$P < 0.05$; **$P < 0.01$; ***$P < 0.001$, Pearson test).

tissues and increased serum amylase and lipase levels compared to the control group. However, Amuc_1100 exerted protective effects against AP risk by decreasing pathological scores and the activities of amylase and lipase in AP mice (Fig. 1b–e). Oral administration of Amuc_1100 also elevated anti-inflammatory capacity by reducing TNF-α, IL-1β, IFN-γ and IL-6 in the pancreatic and splenic tissues of mice (Fig. 1f–i and 2b–e). These results are consistent with previous reports that Amuc_1100 supplementation significantly decreased inflammatory infiltrates and contributed to reduced TNF-α secretion [28]. Amuc_1100 intervention may exert its function by impacting protein levels in the NF-κB signaling pathway (Fig. 1m and 2i). The data suggest that Amuc_1100 attenuated inflammatory properties through inactivation of NF-κB signaling. These results indicate that Amuc_1100 is a potential drug for preventing AP progression.

Macrophages produce proinflammatory cytokines such as TNF-α and IL-6 [29]. Asialoglycoprotein receptor 1 knockdown mice had inhibited Ly6C^{hi} inflammatory monocytes, CD45^{+}CD11b^{hi}F4/80^{+}Ly6C^{lo} monocyte-derived macrophages, CD45^{+}CD11b^{+}F4/80^{+}Ly6C^{+} inflammatory macrophages and the production of TNF-α, IL-1β, and IL-6 in the liver [30]. The infiltration of Ly6C^{hi} macrophages in pancreatic tissues significantly increased in the early stage of AP after partial ligation of duct injury [31]. In our study, we found that the percentage of macrophages increased in the spleen of AP mice, while oral administration of Amuc_1100 significantly decreased this proportion (Fig. 3a). Moreover, Amuc_1100 reduced the number of Ly6C^{+}

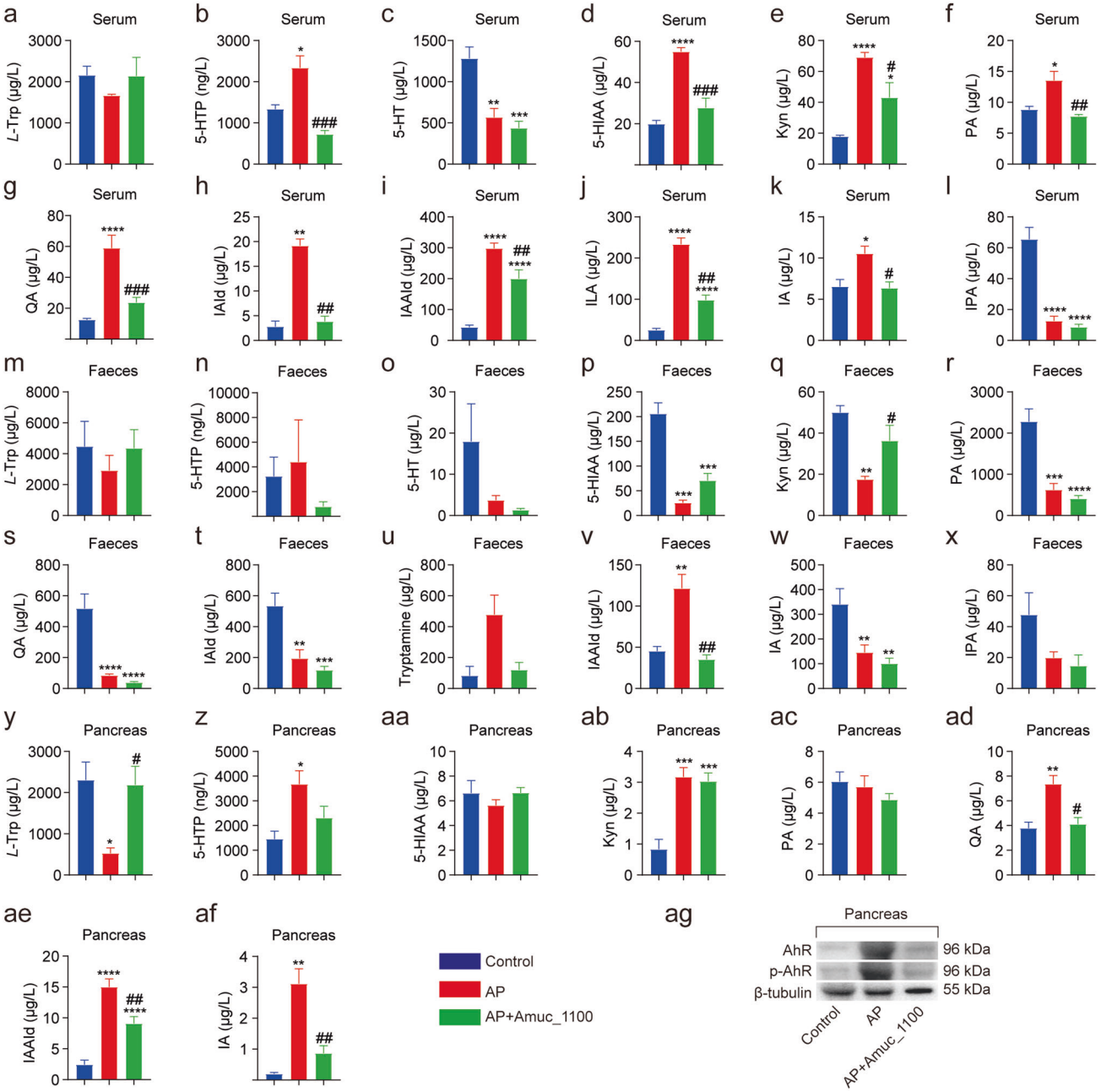

Fig. 7 The effect of Amuc_1100 on Trp metabolism in the serum, feces and pancreas of mice with AP. The metabolites in serum (**a–l**), feces (**m–x**) and pancreas (**y–af**) from AP mice induced by caerulein and LPS with or without Amuc_1100. Quantification of tryptophan metabolites was performed using UHPLC-MS, including *L*-Trp, 5-HTP, 5-HT, 5-HIAA, Kyn, PA, QA, ILA, IA, IPA, tryptamine, IAAld, and IAld. **ag** The protein expression and phosphorylation levels of aryl hydrocarbon receptor (AhR) were analyzed by standard Western blotting methods. β-tubulin was used as an internal reference. Data are provided as the mean ± SEM and were analyzed by one-way ANOVA and Tukey's multiple comparisons test. $^{*}P < 0.05$; $^{**}P < 0.01$; $^{***}P < 0.001$; $^{****}P < 0.0001$, compared with Control. $^{\#}P < 0.05$; $^{\#\#}P < 0.01$; $^{\#\#\#}P < 0.001$, compared to AP mice.

inflammatory macrophages (Fig. 3c). The altered expression of PD-1 in macrophages (Fig. 3b) and Ly6C^{+} macrophages (Fig. 3d) was not detected in the spleen of AP mice. Blood β-hydroxybutyrate treatment increased the production of proinflammatory cytokines, including TNF-α, IL-1β, and IL-6 in bovine neutrophils [32]. Our results demonstrated greater neutrophil concentration and decreased expression of PD-1 in the spleen of AP mice compared to the controls, while oral administration of Amuc_1100 reversed this trend (Fig. 3e-f). Ultimately, Amuc_1100 improved the population and function of macrophages and neutrophils in AP mice.

AP can cause damage to the gut barrier, and the severity of this damage is influenced by the composition of intestinal flora [33, 34]. To treat AP, oral administration of prebiotics, synbiotics, and probiotics has been used to maintain gut microbiota balance, effectively decreasing hospitalization, morbidity and mortality in the early phase of AP [9]. *A. muciniphila*, a widely recognized beneficial microbe, interacts with host signaling pathways to regulate the homeostasis and barrier integrity of the gastrointestinal tract [35]. The supplementation of membrane protein Amuc_1100, derived from *A. muciniphila*, can improve the function of intestinal flora and the abundance of *A. muciniphila* in the intestine [36]. Hence,

Amuc_1100 was used to validate its effect on gut microbiota in the development of AP. Herein, Amuc_1100 treatment did not shift alpha diversity in the cecal contents of AP mice, but it altered the proportion of intestinal flora (Fig. 4a, b). Previous reports have shown that the *Firmicutes*/*Bacteroidetes* (F/B) ratio was increased in the severe AP group [37], and reduced *Actinobacteria* was related to neutrophils in patients with severe AP compared to healthy controls [38]. Additionally, there was a positive association between *Campylobacter* infection and AP incidence [39]. Oral supplementation of Amuc_1100 reduced the abundance of *Bacteroidota*, *Proteobacteria*, *Desulfobacterota* and *Campilobacterota* in AP mice, while it increased the percentage of *Firmicutes* and *Actinobacteriota* (Fig. 4c–i). These findings suggest that the protective effects of Amuc_1100 on AP depend on the microbiota. Notably, *Desulfobacterota* may be a novel target for AP intervention.

The intestinal microbiome is a hidden metabolic organ, providing biochemical pathways that are absent in humans [40]. Potential therapy strategies targeted tryptophan biosynthesis and metabolism in AP [41]. In the present study, metabolic profiling of serum samples from mice revealed the enrichment of tryptophan metabolism (Fig. 5), which was confirmed by KEGG enrichment analysis (Supplementary Fig. 6). Tryptophan, an essential amino acid and a biosynthetic precursor of microorganisms and metabolites, is involved in gut inflammation, intestinal barrier function and energy homeostasis of the host [42, 43]. Early tryptophan depletion paralleled AP severity and systemic inflammation [44]. The results of this study showed that supplementation with Amuc_1100 improved tryptophan metabolism (Fig. 5). Furthermore, correlation analysis of metabolic profiling and intestinal flora showed that the richness values of *Parabacteroides*, *Roseburia*, *Desulfovibrionaceae* and *Ruminococcaceae* were positively correlated with indolelactic acid, while they were negatively related to *L*-tryptophan levels in AP mice *vs* Amuc_1100 treatment (Fig. 6). AhR is activated by Trp metabolites including IA, IPA, IAld, IAA and IAAld. Amuc_1100 could upregulate the expression of AhR in AP, suggesting that Amuc_1100 might trigger AhR signaling through decreasing IAAld and IA (Fig. 7). Oral administration of Amuc_1100 attenuated pancreatic injuries and elevated the level of tryptophan, providing evidence that Amuc_1100 can ameliorate the severity of AP through tryptophan metabolism.

This study highlights the protective role of Amuc_1100 in AP as a critical regulator of intestinal flora and metabolism. Amuc_1100 treatment was found to reshape the immune landscape to blunt inflammation-associated AP. These findings suggest that Amuc_1100 may be a promising therapeutic target in AP.

ACKNOWLEDGEMENTS

The authors acknowledge the science and technology experiment center in Nanjing University of Chinese Medicine for flow cytometry.

AUTHOR CONTRIBUTIONS

WL and LJW directed the research and wrote the manuscript. LJW designed the experiments and WLP analyzed the data. YLJ carried out most of the experiments. JCL helped with raising mice. HE staining was carried out by RLZ. JJW performed some Western blot experiments.

FUNDING

This project was financially supported by the National Natural Science Foundations of China (No. 32270192 and 82072240), the Open Funding Project of the State Key Laboratory of Bioreactor Engineering, the Open Project of the State Key Laboratory of Drug Research, Shanghai Institute of Materia Medica, Chinese Academy of Sciences (No. SIMM2205KF-15), the Open Project of Chinese Materia Medica First-Class Discipline of Nanjing University of Chinese Medicine (No. 2020YLXK008), the Natural Science Foundation of Jiangsu Province of China (BK20230064 to WL), the Fok Ying Tung Education Foundation (No. 171033 to WL), high level key discipline construction project of the National Administration of Traditional Chinese Medicine-Resource Chemistry of Chinese Medicinal Materials (No. zyyzdxk-2023083 to WL).

ADDITIONAL INFORMATION

Supplementary information The online version contains supplementary material available at https://doi.org/10.1038/s41401-023-01186-4.

Competing interests: The authors declare no competing interests.

REFERENCES

1. Gardner TB. Acute pancreatitis. Ann Intern Med. 2021;174:17–32.
2. Forsmark CE, Vege SS, Wilcox CM. Acute pancreatitis. N Engl J Med. 2016;375:1972–81.
3. Krishna SG, Kamboj AK, Hart PA, Hinton A, Conwell DL. The changing epidemiology of acute pancreatitis hospitalizations: a decade of trends and the impact of chronic pancreatitis. Pancreas. 2017;46:482–8.
4. Lankisch PG, Apte M, Banks PA. Acute pancreatitis. Lancet. 2015;386:85–96.
5. Boxhoorn L, Voermans RP, Bouwense SA, Bruno MJ, Verdonk RC, Boermeester MA, et al. Acute pancreatitis. Lancet. 2020;396:726–34.
6. Banks PA, Bollen TL, Dervenis C, Gooszen HG, Johnson CD, Sarr MG, et al. Classification of acute pancreatitis-2012: revision of the Atlanta classification and definitions by international consensus. Gut. 2013;62:102–11.
7. Vege SS, DiMagno MJ, Forsmark CE, Martel M, Barkun AN. Initial medical treatment of acute pancreatitis: American Gastroenterological Association Institute Technical Review. Gastroenterology. 2018;154:1103–39.
8. Mederos MA, Reber HA, Girgis MD. Acute pancreatitis: a review. JAMA. 2021;325:382–90.
9. Patel BK, Patel KH, Bhatia M, Iyer SG, Madhavan K, Moochhala SM. Gut microbiome in acute pancreatitis: A review based on current literature. World J Gastroenterol. 2021;27:5019–36.
10. Schmitt FCF, Brenner T, Uhle F, Loesch S, Hackert T, Ulrich A, et al. Gut microbiome patterns correlate with higher postoperative complication rates after pancreatic surgery. BMC Microbiol. 2019;19:42.
11. Malla MA, Dubey A, Kumar A, Yadav S, Hashem A, Abd Allah EF. Exploring the human microbiome: the potential future role of next-generation sequencing in disease diagnosis and treatment. Front Immunol. 2018;9:2868.
12. Sanger F, Coulson AR. A rapid method for determining sequences in DNA by primed synthesis with DNA polymerase. J Mol Biol. 1975;94:441–8.
13. Tan C, Ling Z, Huang Y, Cao Y, Liu Q, Cai T, et al. Dysbiosis of intestinal microbiota associated with inflammation involved in the progression of acute pancreatitis. Pancreas. 2015;44:868–75.
14. Rychter JW, van Minnen LP, Verheem A, Timmerman HM, Rijkers GT, Schipper ME, et al. Pretreatment but not treatment with probiotics abolishes mouse intestinal barrier dysfunction in acute pancreatitis. Surgery. 2009;145:157–67.
15. Zhu Y, He C, Li X, Cai Y, Hu J, Liao Y, et al. Gut microbiota dysbiosis worsens the severity of acute pancreatitis in patients and mice. J Gastroenterol. 2019;54:347–58.
16. Plovier H, Everard A, Druart C, Depommier C, Van Hul M, Geurts L, et al. A purified membrane protein from *Akkermansia muciniphila* or the pasteurized bacterium improves metabolism in obese and diabetic mice. Nat Med. 2017;23:107–13.
17. Ottman N, Reunanen J, Meijerink M, Pietilä TE, Kainulainen V, Klievink J, et al. Pili-like proteins of *Akkermansia muciniphila* modulate host immune responses and gut barrier function. PLoS One. 2017;12:e0173004.
18. Wang J, Xiang R, Wang R, Zhang B, Gong W, Zhang J, et al. The variable oligomeric state of Amuc_1100 from *Akkermansia muciniphila*. J Struct Biol. 2020;212:107593.
19. Wang L, Tang L, Feng Y, Zhao S, Han M, Zhang C, et al. A purified membrane protein from *Akkermansia muciniphila* or the pasteurised bacterium blunts colitis associated tumourigenesis by modulation of $CD8^+$ T cells in mice. Gut. 2020;69:1988–97.
20. Mulhall H, DiChiara JM, Deragon M, Iyer R, Huck O, Amar S. *Akkermansia muciniphila* and its pili-like protein Amuc_1100 modulate macrophage polarization in experimental periodontitis. Infect Immun. 2020;89:e00500–20.
21. Wang J, Xu W, Wang R, Cheng R, Tang Z, Zhang M. The outer membrane protein Amuc_1100 of *Akkermansia muciniphila* promotes intestinal 5-HT biosynthesis and extracellular availability through TLR2 signalling. Food Funct. 2021;12:3597–610.
22. Cani PD, Knauf C. A newly identified protein from *Akkermansia muciniphila* stimulates GLP-1 secretion. Cell Metab. 2021;33:1073–5.
23. Cani PD, de Vos WM. Next-generation beneficial microbes: the case of *Akkermansia muciniphila*. Front Microbiol. 2017;8:1765.
24. Kusske AM, Rongione AJ, Ashley SW, McFadden DW, Reber HA. Interleukin-10 prevents death in lethal necrotizing pancreatitis in mice. Surgery. 1996;120:284–8.

25. Salminen A, Huuskonen J, Ojala J, Kauppinen A, Kaarniranta K, Suuronen T. Activation of innate immunity system during aging: NF-κB signaling is the molecular culprit of inflamm-aging. Ageing Res Rev. 2008;7:83–105.
26. Piao X, Liu B, Sui X, Li S, Niu W, Zhang Q, et al. Picroside II improves severe acute pancreatitis-induced intestinal barrier injury by inactivating oxidative and inflammatory TLR4-dependent PI3K/AKT/NF-κB signaling and improving gut microbiota. Oxid Med Cell Longev. 2020;2020:3589497.
27. Liu K, Yang L, Wang X, Huang Q, Tuerhong K, Yang M, et al. Electroacupuncture regulates macrophage, neutrophil, and oral microbiota to alleviate alveolar bone loss and inflammation in experimental ligature-induced periodontitis. J Clin Periodontol. 2023;50:368–79.
28. Mulhall H, DiChiara JM, Huck O, Amar S. Pasteurized *Akkermansia muciniphila* reduces periodontal and systemic inflammation induced by *Porphyromonas gingivalis* in lean and obese mice. J Clin Periodontol. 2022;49:717–29.
29. Xu X, Qiao Y, Peng Q, Dia VP, Shi B. Probiotic activity of ropy *Lactiplantibacillus plantarum* NA isolated from Chinese northeast sauerkraut and comparative evaluation of its live and heat-killed cells on antioxidant activity and RAW 264.7 macrophage stimulation. Food Funct. 2023;14:2481–95.
30. Shi R, Wang J, Zhang Z, Leng Y, Chen AF. ASGR1 promotes liver injury in sepsis by modulating monocyte-to-macrophage differentiation via NF-κB/ATF5 pathway. Life Sci. 2023;315:121339.
31. Van Gassen N, Van Overmeire E, Leuckx G, Heremans Y, De Groef S, Elkrim Y, et al. Macrophage dynamics are regulated by local macrophage proliferation and monocyte recruitment in injured pancreas. Eur J Immunol. 2015;45:1482–93.
32. He J, Wang K, Liu M, Zeng W, Li D, Majigsuren Z, et al. β-hydroxybutyrate enhances bovine neutrophil adhesion by inhibiting autophagy. Front Immunol. 2022;13:1096813.
33. Rahman SH, Ammori BJ, Holmfield J, Larvin M, McMahon MJ. Intestinal hypoperfusion contributes to gut barrier failure in severe acute pancreatitis. J Gastrointest Surg. 2003;7:26–36.
34. Zhang D, Zhu C, Fang Z, Zhang H, Yang J, Tao K, et al. Remodeling gut microbiota by *Clostridium butyricum* (*C. butyricum*) attenuates intestinal injury in burned mice. Burns. 2020;46:1373–80.
35. Shin J, Noh JR, Chang DH, Kim YH, Kim MH, Lee ES, et al. Elucidation of *Akkermansia muciniphila* probiotic traits driven by mucin depletion. Front Microbiol. 2019;10:1137.
36. Dong X, Liu M, Liu X, Liu M, Zhang X, Wang G. Prokaryotic expression of Amuc_1100 protein and its effects on high-fat diet rats combined streptozotocin injection. Wei Sheng Yan Jiu. 2020;49:785–822.
37. Liu J, Luo M, Qin S, Li B, Huang L, Xia X. Significant succession of intestinal bacterial community and function during the initial 72 h of acute pancreatitis in rats. Front Cell Infect Microbiol. 2022;12:808991.
38. Li Q, Wang C, Tang C, Zhao X, He Q, Li J. Identification and characterization of blood and neutrophil-associated microbiomes in patients with severe acute pancreatitis using next-generation sequencing. Front Cell Infect Microbiol. 2018;8:5.
39. Oh SJ, Pimentel M, Leite GGS, Celly S, Villanueva-Millan MJ, Lacsina I, et al. Acute appendicitis is associated with appendiceal microbiome changes including elevated *Campylobacter jejuni* levels. BMJ Open Gastroenterol. 2020;7:e000412.
40. Khan I, Yasir M, Azhar EI, Kumosani T, Barbour EK, Bibi F, et al. Implication of gut microbiota in human health. CNS Neurol Disord Drug Targets. 2014;13:1325–33.
41. Guo J, Li X, Wang D, Guo Y, Cao T. Exploring metabolic biomarkers and regulation pathways of acute pancreatitis using ultra-performance liquid chromatography combined with a mass spectrometry-based metabolomics strategy. RSC Adv. 2019;9:12162–73.
42. Zhang K, Li X, Wang X, Zheng H, Tang S, Lu L, et al. Gut barrier proteins mediate liver regulation by the effects of serotonin on the non-alcoholic fatty liver disease. Curr Protein Pept Sci. 2020;21:978–84.
43. Li X, Zhang ZH, Zabed HM, Yun J, Zhang G, Qi X. An insight into the roles of dietary tryptophan and its metabolites in intestinal inflammation and inflammatory bowel disease. Mol Nutr Food Res. 2021;65:e2000461.
44. Skouras C, Zheng X, Binnie M, Homer NZ, Murray TB, Robertson D, et al. Increased levels of 3-hydroxykynurenine parallel disease severity in human acute pancreatitis. Sci Rep. 2016;6:33951.

Springer Nature or its licensor (e.g. a society or other partner) holds exclusive rights to this article under a publishing agreement with the author(s) or other rightsholder(s); author self-archiving of the accepted manuscript version of this article is solely governed by the terms of such publishing agreement and applicable law.